Inorg. Chem. **2006**, *45*, 5980–5988

Synthesis and Characterization of Metal–Organic Frameworks Based on 4-Hydroxypyridine-2,6-dicarboxylic Acid and Pyridine-2,6-dicarboxylic Acid Ligands

Hong-Ling Gao,[†,‡] Long Yi,[†] Bin Zhao,[†] Xiao-Qing Zhao,[†] Peng Cheng,*[,†] Dai-Zheng Liao,[†] and Shi-Ping Yan[†]

Department of Chemistry, Nankai University, Tianjin 300071, P. R. China, and Department of Chemistry, Tianjin University, Tianjin 300072, P. R. China

Received April 2, 2006

The self-assembly of 4-hydroxypyridine-2,6-dicarboxylic acid (H_3CAM) and pyridine-2,6-dicarboxylic acid (H_2PDA) with Zn(II) salts under hydrothermal conditions gave two novel coordination polymers $\{[Zn(HCAM)]\cdot H_2O\}_n$ (**1**) and $\{[Zn(PDA)(H_2O)_{1.5}]\}_n$ (**1a**). **1** and **1a** comprise of a 2D (4,4) net and a 1D zigzag chain, respectively, in which a new coordination mode of PDA is found. The reactions of H_3CAM and H_2PDA with Nd_2O_3 in the M/L ratio 2:3 gave $\{[Nd_2(HCAM)_3(H_2O)_4]\cdot 2H_2O\}_n$ (**2**) and $\{[Nd_2(PDA)_3(H_2O)_3]\cdot 0.5H_2O\}_n$ (**2a**). In **2**, a square motif as a building block constructed by four Nd(III) ions was further assembled into a highly ordered 2D (4,4) grid. **2a** is a 3D microporous coordination polymer. It is interesting to note that, when Ln(III) salts rather than oxides were employed, the reaction produced $\{[Ln(CAM)(H_2O)_3]\cdot H_2O\}_n$ (Ln = Gd, **3**; Dy, **4**; Er, **5**) for H_3CAM and $\{[Gd_2(PDA)_3(H_2O)_3]\cdot H_2O\}_n$ (**3a**) for H_2PDA. **3**–**5** are 2D coordination polymers with a 3^34^2 uniform net, where hydroxyl groups of H_3CAM coordinate with metal ions. The reaction of H_3CAM and Er_2O_3 instead of $Er(ClO_4)_3$ produced $\{[Er_2(HCAM)_3(H_2O)_4]\cdot 2H_2O\}_n$ (**6**). The compounds **2a** and **3a**, **2** and **6** are isomorphous. The stereochemical and supramolecular effects of hydroxyl groups result in the dramatic structural changes from 1D (**1a**) to 2D (**1**) and from 2D (**2**) to 3D (**2a**). When Ln(III) salts instead of Ln_2O_3 were employed in the hydrothermal reactions with H_3CAM, different self-assembly processes gave the products of different metal/ligand ratio with reactants (**3**–**5**).

Introduction

The study of coordination polymers has gained great recognition as an important interface between synthetic chemistry and materials science and provides a solid foundation for understanding how molecules can be organized and how functions can be achieved. The current topical areas focus on the construction of metal−organic frameworks (MOFs) with novel topology and on the crystal engineering of molecular architectures organized by coordination bonds and supramolecular contacts (such as hydrogen bonding, $\pi-\pi$ interactions, etc.).[1−10] Thus, many spectacular MOFs have been documented, such as 1D chains[11] and ladders,[12] 2D grids,[13] 3D microporous networks,[14] interpenetrated modes,[15] and helical staircase networks,[16] which are likely used as new materials, such as molecular magnets, opto-

* To whom correspondence should be addressed. E-mail: pcheng@nankai.edu.cn. Tel: +86-22-23509957. Fax: +86-22-23502458.
[†] Nankai University.
[‡] Tianjin University.

(1) Fujita, M.; Oka, H.; Yamaguchi, K.; Ogura, K. *Nature* **1995**, *378*, 469.
(2) (a) Moulton, B.; Zaworotko, M. J. *Chem. Rev.* **2001**, *101*, 1629. (b) Evans, O. R.; Lin, W. B. *Acc. Chem. Res.* **2002**, *35*, 511.
(3) (a) Hoskins, B. F.; Robson, R.; Slizys, D. A. *J. Am. Chem. Soc.* **1997**, *119*, 2952. (b) Hoskins, B. F.; Robson, R.; Slizys, D. A. *Angew. Chem., Int. Ed.* **1997**, *36*, 2336.
(4) (a) Zhao, B.; Cheng, P.; Dai Y.; Cheng C.; Liao, D. Z.; Yan, S. P.; Jiang, Z. H.; Wang, G. L. *Angew. Chem., Int. Ed.* 2003, *42*, 934. (b) Zhao, B.; Cheng, P.; Chen X.; Cheng, C.; Shi, W.; Liao, D. Z.; Yan, S. P.; Jiang, Z. H. *J. Am. Chem.* Soc. **2004**, *126*, 3012.
(5) Kitaura, R.; Seki. K.; Akiyama, G.; Kitagawa, S. *Angew. Chem., Int. Ed*. **2003**, *42*, 428.
(6) Kasai, M.; Aoyagi, M.; Fujita, M. *J. Am. Chem. Soc.* **2000**, *122*, 2140.
(7) Campos-Fernandez, C. S.; Schottel, B. L.; Chifotides, H. T.; Bera, J. K.; Bacsa, J.; Koomen, J. M.; Russell, D. H.; Dunbar, K. R. *J. Am. Chem. Soc*. **2005**, *127*, 12909.
(8) Goher, M. A. S.; Mautner, F. A.; Youssef, M. A. M. A.; Hafez K. A.; Badr A. M. A. *Dalton Trans.* **2002**, 3309.
(9) Zhang, L.; Cheng, P.; Tang, L. F.; Weng, L. H.; Jiang, Z. H.; Liao, D. Z.; Yan, S. P.; Jiang, Z. H.; Wang, G. L. *Chem. Commun*. **2000**, 717.
(10) Yi, L.; Ding, B.; Zhao, B.; Cheng, P.; Liao, D. Z.; Yan, S. P.; Jiang, Z. H. *Inorg. Chem.* **2004**, *43*, 33.
(11) Yi, L.; Yang, X.; Cheng, P.; Lu, T. B. *Cryst. Growth Des.* **2005**, *5*, 1215.

10.1021/ic060550j CCC: $33.50
Published on Web 06/28/2006

Scheme 1. Known Coordination Modes of PDA and CAM

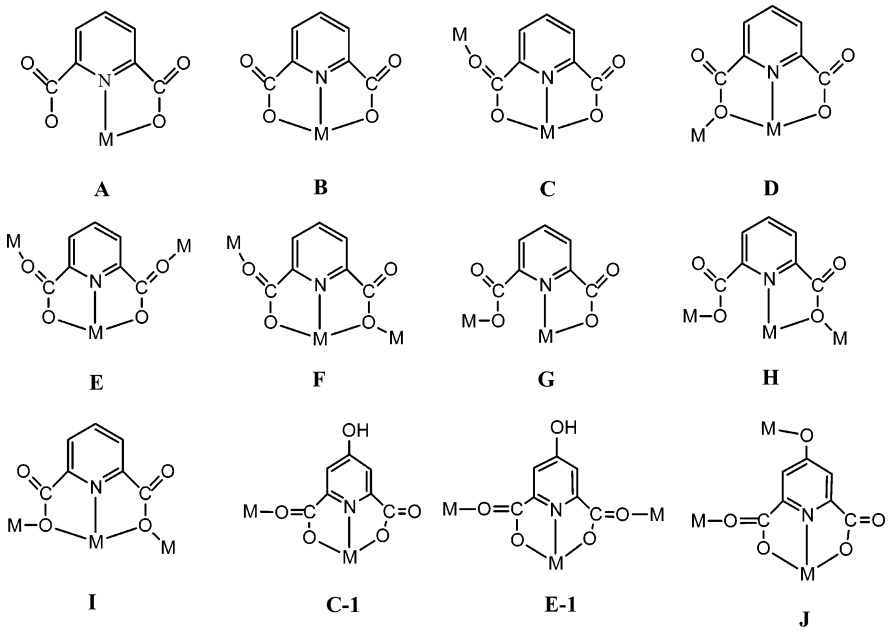

electronic devices, sensors, catalysts, and so on.[17−26] In our previous work, a successful synthetic strategy by tuning the Pr/ligand ratios (from 1:2 and 3:5 to 3:4) to control the structures was applied under the same reaction conditions (hydrothermal synthesis), and coordination polymers from 1D and 2D to 3D, respectively, were isolated with Pr/ligand ratios of 1:2, 3:5, and 2:3 in the structures.[27a] Recent research concerns the influence of water content on the topologies of MOFs that are self-assembled from pyridine-3,5-dicarboxylate and divalent metal ions under mild conditions.[27b] However, the control of the orientation and stereochemistry of the building units in the solid state continue to be an obstacle in the preparation of a given molecular topology and architecture. The controlling factors and the experimental conditions for the preparation of MOFs are not completely understood.

On the other hand, it is well known that carboxylate ligands play an important role to construct novel MOFs in coordination chemistry. They usually adopt binding modes diverse as terminal monodentate, chelating to one metal center, bridging didentate in a syn−syn, syn−anti, and anti−anti configuration to two metal centers, and bridging tridentate to two metal centers.[28] A large number of MOFs containing carboxylate ligands have been prepared, and almost all of them are in polymeric forms.[2,4,29] Pyridine-2,6-dicarboxylic acid (H_2PDA) as a very important carboxylate derivative has attracted much interest in coordination chemistry. H_2PDA has a rigid 120° angle between the central pyridine ring and two carboxylate groups and therefore could potentially provide various coordination motifs to form both discrete and consecutive metal complexes under appropriate synthesis condition.[27a] A systematic study of 3d, 4f, 3d−4f, 4d−4f, and 3d−4d complexes based on H_2PDA has been undertaken in our lab[4,27a,30] which gives rich coordination motifs for PDA (Scheme 1). 4-Hydroxypyridine-2,6-dicarboxylic acid (H_3CAM) unites the coordination geometry of H_2PDA and a hydroxyl group, which can potentially provide more coordination motifs than H_2PDA.

(12) Withersby, M. A.; Blake, A. J.; Champness, N. R.; Cooke, P. A.; Hubberstey, P.; Li, W. S.; Schröder, M. *Inorg. Chem.* **1999**, *38*, 2259.
(13) Mitsurs, K.; Shimamura, M.; Noro, S. I.; Minakoshi, S.; Asami, A.; Seki, K.; Kitagawa, S. *Chem. Mater.* **2000**, *12*, 1288.
(14) (a) Pan, L.; Sander, M. B.; Huang, X.; Li, J.; Smith, M.; Bittner, E.; Bockrath, B.; Johnson, J. K. *J. Am. Chem. Soc.* **2004**, *126*, 1308. (b) Gao, H. L.; Yi, L.; Ding, B.; Wang, H. S.; Cheng, P.; Liao, D. Z.; Yan, S. P. *Inorg. Chem.* **2006**, *45*, 481.
(15) Hill, R. J.; Long, D.-L.; Champness, N. R.; Hubberstey, P.; Schröder, M. *Acc. Chem. Res.* **2005**, *38*, 335.
(16) Maggard, P. A.; Stern, C. L.; Poeppelmeier, K. R. *J. Am. Chem. Soc.* **2001**, *123*, 7742.
(17) Fujita, M.; Kwon, Y. J. *J. Am. Chem. Soc.* **1994**, *116*, 1151.
(18) Chui, S. S.-Y.; Lo, S. M.-F.; Charmant, J. P. H.; Orphen, A. G.; Williams, I. D. *Science* **1999**, *283*, 1148.
(19) Berlinguette, C. P.; Dragulescu-Andrasi, A.; Sieber, A.; Galan-Mascaros, J. R.; Gudel, H.-U.; Achim, C.; Dunbar, K. R. *J. Am. Chem. Soc.* **2004**, *126*, 6222.
(20) Palii, A. V.; Ostrovsky, S. M.; Klokishner, S. I.; Tsukerblat, B. S.; Berlinguette, C. P.; Dunbar, K. R.; Galan-Mascaros, J. R. *J. Am. Chem. Soc.* **2004**, *126*, 16860.
(21) Leadbeater, N. E.; Marco, M. *Chem. Rev.* **2002**, *102*, 3217.
(22) Skovic, C.; Colette, B.; Euan, K.; Streib, W. E.; Folting, K.; Bollinger, J. C.; Hendrickson, D. N.; Christou, G. *J. Am. Chem. Soc.* **2002**, *124*, 3725.
(23) Davis, M. E. *Nature* **2002**, *417*, 813.
(24) Tsuchida, E.; Oyaizu. K. *Coord. Chem. Rev.* **2003**, *237*, 213.
(25) (a) Chifotides, H. T.; Dunbar, K. R. *Acc. Chem. Res.* **2005**, *38*, 146. (b) Tsukube, H.; Shinoda, S. *Chem. Rev.* **2002**, *102*, 2389.
(26) Lwamoto, M.; Furukawa, H.; Mine, Y.; Uemura, F.; Mikuriya, S. I.; Kagawa, S. *J. Chem. Soc., Chem. Commun.* **1986**, 1272.
(27) (a) Zhao, B.; Yi, L.; Dai, Y.; Chen, X. Y.; Cheng, P.; Liao, D. Z.; Yan, S. P.; Jiang, Z. H. *Inorg. Chem.* **2005**, *44*, 911. (b) Lu, Y. L.; Wu, J. Y.; Chan, M. C.; Huang, S. M.; Lin, C. S.; Chiu, T. W.; Liu, Y. H.; Wen, Y. S.; Ueng, C. H.; Chin, T. M.; Hung, C. H.; Lu, K. L. *Inorg. Chem.* **2006**, *45*, 2430.
(28) Policar, C.; Lambert, F.; Cesario, M.; Morgenstern-Badarau, I. *Eur. J. Inorg. Chem.* **1999**, 2201.
(29) (a) Prior, T. J.; Bradshaw. D.; Teat, S. J.; Rosseinsky, M. J. *Chem. Commun.* **2003**, 500. (b) Bourne, S. A.; Lu, J. J.; Mondal, A.; Moulton, B.; Zaworotko, M. J. *Angew. Chem., Int. Ed.* **2001**, *40*, 2111.
(30) (a) Zhao, B.; Gao, H. L.; Chen, X. Y.; Cheng, P.; Shi, W.; Liao, D. Z.; Yan, S. P.; Jiang, Z. H. *Chem. Eur. J.* **2006**, *12*, 149. (b) Zhao, B.; Yi, L.; Cheng, P.; Liao, D. Z.; Yan, S. P.; Jiang, Z. H. *Inorg. Chem. Commun.* **2004**, *7*, 971. (c) Zhao, B.; Chen, X. Y.; Cheng, P.; Liao, D. Z.; Yan, S. P.; Jiang, Z. H. *J. Am. Chem. Soc.* **2004**, *126*, 15394.

This contribution first contrastively studies on the coordination chemistry of H_3CAM and H_2PDA in different complexes under hydrothermal conditions. Herein a series of coordination polymers, $\{[Zn(HCAM)]\cdot H_2O\}_n$ (**1**), $\{[Zn(PDA)(H_2O)_{1.5}]\}_n$ (**1a**), $\{[Ln_2(HCAM)_3(H_2O)_4]\cdot 2H_2O\}_n$ (Ln = Nd, **2**; Er, **6**), $\{[Nd_2(PDA)_3(H_2O)_3]\cdot 0.5H_2O\}_n$ (**2a**), $\{[Ln(CAM)(H_2O)_3]\cdot H_2O\}_n$ (Ln = Gd, **3**; Dy, **4**; Er, **5**), and $\{[Gd_2(PDA)_3(H_2O)_3]\cdot H_2O\}_n$ (**3a**) were isolated under hydrothermal conditions and characterized by elemental analyses, IR, TGA, photoluminescence measurements, magnetic susceptibilities, and single-crystal X-ray diffraction analyses.

Experiment Section

Materials. All chemicals purchased were reagent grade and used without further purification. Elemental analyses (C, H, and N) were performed on a Perkin-Elmer 240 CHN elemental analyzer. IR spectra were recorded in the range 400−4000 cm^{-1} on a Bruker TENOR 27 spectrophotometer using a KBr pellet. TGA experiments were performed on a NETZSCH TG 209 instrument with a heating rate of 5 °C min^{-1}. The photoluminescence spectrum was measured by a MPF-4 fluorescence spectrophotometer with a xenon arc lamp as the light source. Variable-temperature magnetic susceptibilities were measured on a Quantum Design MPMS-7 SQUID magnetometer. Diamagnetic corrections were made with Pascal's constants for all the constituent atoms.

Preparations. $\{$**[Zn(HCAM)]·H$_2$O**$\}_n$ **(1). 1** was synthesized from the reaction mixture of $ZnSO_4$ (0.2 mmol, 0.0485 g), H_3CAM (0.2 mmol, 0.0400 g), H_2O (10 mL), and C_2H_5OH (2 mL) in a 25 mL Teflon reactor, under autogenous pressure at 180 °C for 3 days, and then cooled to room temperature at a rate of 10 °C h^{-1}. Colorless crystals of **2** were obtained (yield: 57% based on Zn). Anal. Found: C 31.45, H 1.76, N 5.66%. Calcd: C 31.79, H 1.91, N 5.30%. IR (KBr): ν = 3598.7s, 3078.5s; 1638.3s, 1622.1vs, 1469.7m, 1314.5m, 1278.9w, 1121.8m, 1044.3s, 976.4m, 919.2m, 818.8s, 753.8s, 648.3w, 540.3m, 477.8m, 436.9w cm^{-1}.

$\{$**[Zn(PDA)(H$_2$O)$_{1.5}$]**$\}_n$ **(1a). 1a** was synthesized from the reaction mixture of $ZnSO_4$ (0.2 mmol, 0.0485 g), H_2PDA (0.2 mmol, 0.0334 g), H_2O (10 mL), and C_2H_5OH (2 mL) in a 25 mL Teflon reactor, under autogenous pressure at 180 °C for 3 days, and then cooled to room temperature at a rate of 10 °C h^{-1}. Colorless crystals of **1a** were obtained (yield: 49% based on Zn). Anal. Found: C, 32.45; H, 2.51; N, 5.47%. Calcd: C, 32.65; H, 2.35; N, 5.44%. IR (KBr): ν = 3430.4bm, 3117.2m, 1614.7vs, 1462.9s, 1396.7s, 1303.9s, 1196.7w, 1156.2w, 1077.9m, 1036.9w, 925.2w, 839.5m, 763.2s, 744.9s, 689.5s, 602.4m, 495.1w, 429.3m cm^{-1}

$\{$**[Nd$_2$(HCAM)$_3$(H$_2$O)$_4$]·2H$_2$O**$\}_n$ **(2). 2** was synthesized from the reaction mixture of Nd_2O_3 (0.2 mmol, 0.0673 g), H_3CAM (0.6 mmol, 0.1206 g), H_2O (10 mL), and C_2H_5OH (2 mL) in a 25 mL Teflon reactor, under autogenous pressure at 180 °C for 3 days, and then cooled to room temperature at a rate of 10 °C h^{-1}. Red crystals of **2** were obtained (yield: 66% based on Nd). Anal. Found: C, 26.45; H, 2.36; N, 4.66%. Calcd: C, 26.84; H, 2.25; N, 4.47%. IR (KBr): ν = 3443.6bs, 1575.7vs, 1427.1s, 1339.4s, 1240.1m, 1124.7m, 1024.8s, 895.0w, 810.1m, 712.1m, 510.8w, 451.9w cm^{-1}.

$\{$**[Nd$_2$(PDA)$_3$(H$_2$O)$_3$]·0.5H$_2$O**$\}_n$ **(2a). 2a** was synthesized from the reaction mixture of Nd_2O_3 (0.2 mmol, 0.0673 g), H_2PDA (0.6 mmol, 0.1003 g), H_2O (10 mL), and C_2H_5OH (2 mL) in a 25 mL Teflon reactor, under autogenous pressure at 180 °C for 3 days, and then cooled to room temperature at a rate of 10 °C h^{-1}. Red crystals of **2a** were obtained (yield: 48% based on Nd). Anal. Found: C, 29.99; H, 2.31; N, 4.66%. Calcd: C, 29.78; H, 1.90; N, 4.96%. IR (KBr): ν = 3574.1s, 3558.0m, 3107.3s, 1621.5vs, 1602.1s, 1582.4s, 1566m, 1467.0w, 1442.3m, 1395.2m, 1375.4s, 1138.1m, 1054.2s, 889.1w, 771.1m, 662.5w, 448.1w cm^{-1}.

$\{$**[Gd(CAM)(H$_2$O)$_3$]·H$_2$O**$\}_n$ **(3). 3** was synthesized from the reaction mixture of $Gd(ClO_4)_3\cdot 6H_2O$ (0.1 mmol, 0.0563 g), H_3CAM (0.15 mmol, 0.0303 g), H_2O (10 mL), and C_2H_5OH (2 mL) in a 25 mL Teflon reactor, under autogenous pressure at 180 °C for 3 days, and then cooled to room temperature at a rate of 10 °C h^{-1}. Crystals of **3** were obtained (yield: 51% based on Gd). Anal. Found: C, 20.45; H, 2.51; N, 3.88%. Calcd: C, 20.54; H, 2.46; N, 3.42%. IR (KBr): ν = 3573.2s, 3211.3bs, 1582.8s, 1435.9s, 1322.2s, 1131.9m, 1033.2s, 895.1w, 817.3m, 734.3s, 459.9m cm^{-1}.

$\{$**[Gd$_2$(PDA)$_3$(H$_2$O)$_3$]·H$_2$O**$\}_n$ **(3a). 3a** was synthesized from the reaction mixture of $Gd(ClO_4)_3\cdot 6H_2O$ (0.1 mmol, 0.0563 g), H_2PDA (0.15 mmol, 0.1003 g), H_2O (10 mL), and C_2H_5OH (2 mL) in a 25 mL Teflon reactor, under autogenous pressure at 180 °C for 3 days, and then cooled to room temperature at a rate of 10 °C h^{-1}. Crystals were obtained (yield: 55% based on Gd). Anal. Found: C, 28.41; H, 1.74; N, 4.05%. Calcd: C, 28.60; H, 1.94; N, 4.76%.

$\{$**[Dy(CAM)(H$_2$O)$_3$]·H$_2$O**$\}_n$ **(4).** 4 was synthesized from the reaction mixture of $DyCl_3\cdot 6H_2O$ (0.1 mmol, 0.0377 g), H_3CAM (0.15 mmol, 0.0301 g), H_2O (10 mL), and C_2H_5OH (2 mL) in a 25 mL Teflon reactor, under autogenous pressure at 180 °C for 3 days, and then cooled to room temperature at a rate of 10 °C h^{-1}. Crystals of **4** were obtained (yield: 41% based on Dy). Anal. Found: C, 20.55; H, 2.35; N, 3.59%. Calcd: C, 20.28; H, 2.43; N, 3.38%.

$\{$**[Er(CAM)(H$_2$O)$_3$]·H$_2$O**$\}_n$ **(5). 5** was synthesized from the reaction mixture of $Er(ClO_4)_3\cdot 6H_2O$ (0.1 mmol, 0.0574 g), H_3CAM (0.15 mmol, 0.0301 g), H_2O (10 mL), and C_2H_5OH (2 mL) in a 25 mL Teflon reactor, under autogenous pressure at 180 °C for 3 days, and then cooled to room temperature at a rate of 10 °C h^{-1}. Crystals of **5** were obtained (yield: 38% based on Er). Anal. Found: C, 20.32; H, 2.77; N, 3.52%. Calcd: C, 20.05; H, 2.40; N, 3.34%.

$\{$**[Er$_2$(HCAM)$_3$(H$_2$O)$_4$]·2H$_2$O**$\}_n$ **(6). 6** was synthesized from the reaction mixture of Er_2O_3 (0.2 mmol, 0.0765 g), H_3CAM (0.6 mmol, 0.1206 g), H_2O (10 mL), and C_2H_5OH (2 mL) in a 25 mL Teflon reactor, under autogenous pressure at 180 °C for 3 days, and then cooled to room temperature at a rate of 10 °C h^{-1}. Crystals of **6** were obtained (yield: 69% based on Er). Anal. Found: C, 26.07; H, 2.43; N, 4.49%. Calcd: C, 25.58; H, 2.15; N, 4.26%.

Crystal Structure Determination. Diffraction intensities for nine complexes were collected on a computer-controlled Bruker SMART 1000 CCD diffractometer equipped with graphite-monochromated Mo Kα radiation with a radiation wavelength of 0.71071 Å by using the ω-scan technique. Lorentz polarization and absorption corrections were applied. The structures were solved by direct methods and refined with full-matrix least-squares technique using the SHELXS-97 and SHELXL-97 programs.[31] Anisotropic thermal parameters were assigned to all non-hydrogen atoms. The organic hydrogen atoms were generated geometrically; the hydrogen atoms of the water molecules were located from difference maps and refined with isotropic temperature factors. Analytical expressions of neutral-atom scattering factors were employed, and anomalous dispersion corrections were incorporated. The crystallographic data for **1**−**6** are listed in Tables 1 and 2.

(31) (a) Sheldrick, G. M. *SHELXL-97, Program for the Solution of Crystal Structures*; University of Göttingen: Göttingen, Germany 1997. (b) Sheldrick, G. M. *SHELXL-97, Program for the Refinement of Crystal Structures*; University of Göttingen: Göttingen, Germany, 1997.

Table 1. Crystal Data and Structure Refinement Information for Compounds **1**−**2a**

compounds	**1**	**1a**	**2**	**2a**
formula	$C_7H_5NO_6Zn$	$C_7H_6NO_{5.5}Zn$	$C_{21}H_{21}N_3Nd_2O_{21}$	$C_{21}H_{16}N_3Nd_2O_{15.5}$
fw	263.48	257.50	939.89	846.85
temp (K)	293(2)	273(2)	293(2)	293(2)
cryst syst	tetragonal	monoclinic	monoclinic	monoclinic
space group	$P\bar{4}2(1)c$	$C2/c$	$P2(1)/n$	$P2(1)/c$
a (Å)	10.0228(19)	13.252(4)	9.673(3)	11.026(14)
b (Å)	10.0228(19)	9.769(3)	13.622(4)	17.54(2)
c (Å)	16.583(6)	13.174(4)	22.292(6)	13.472(18)
β (°)		96.259(6)	93.103(4)	100.93(2)
V (Å^3)	1665.8(8)	1695.3(10)	2933.0(14)	2558(6)
Z	8	8	4	4
F(000)	1048	1032	1824	1628
ρ (Mg/m^3)	2.101	2.018	2.128	2.199
abs coeff (mm^{-1})	2.957	2.899	3.600	4.099
GOF	1.108	1.101	1.157	1.014
R1[a] ($I = 2\sigma$(I))	0.0399	0.0588	0.0230	0.0371
WR2[a] (all data)	0.0939	0.1831	0.0641	0.1033

[a] $R1 = \Sigma||F_o| - |F_c||/|F_o|$, $wR2 = [\Sigma w(F_o^2 - F_c^2)^2/\Sigma w(F_o^2)^2]^{1/2}$.

Table 2. Crystal Data and Structure Refinement Information for Compounds **3**−**6**

compounds	**3**	**3a**	**4**	**5**	**6**
formula	$C_7H_{10}GdNO_9$	$C_{21}H_{17}Gd_2N_3O_{16}$	$C_7H_{10}DyNO_9$	$C_7H_{10}ErNO_9$	$C_{21}H_{21}Er_2N_3O_{21}$
fw	409.41	881.88	414.66	419.42	985.93
temp (K)	293(2)	293(2)	293(2)	293(2)	294(2)
cryst syst	monoclinic	monoclinic	monoclinic	monoclinic	monoclinic
space group	$P2(1)/n$	$P2(1)/c$	$P2(1)/n$	$P2(1)/c$	$P2(1)/n$
a (Å)	9.980(3)	10.906(3)	9.907(3)	9.874(9)	8.9725(15)
b (Å)	7.562(2)	17.443(5)	7.542(2)	7.559(7)	14.537(2)
c (Å)	15.522(4)	13.201(4)	15.429(4)	15.387(14)	21.710(4)
β (°)	104.96	101.627(4)	105.236(4)	105.509(11)	90.903(3)
V (Å^3)	1131.6(5)	2459.9(13)	1112.3(5)	1106.6(18)	2831.4(8)
Z	4	4	4	4	4
F(000)	780	1680	788	796	1888
ρ (Mg/m^3)	2.403	2.381	2.476	2.518	2.313
abs coeff (mm^{-1})	5.903	5.436	6.761	7.627	5.989
GOF	1.078	1.095	1.165	1.042	1.004
R1[a] ($I = 2\sigma$(I))	0.0205	0.0177	0.0190	0.0466	0.0291
WR2[a] (all data)	0.0527	0.0407	0.0485	0.1627	0.0664

[a] $R1 = \Sigma||F_o| - |F_c||/|F_o|$, $wR2 = [\Sigma w(F_o^2 - F_c^2)^2/\Sigma w(F_o^2)^2]^{1/2}$.

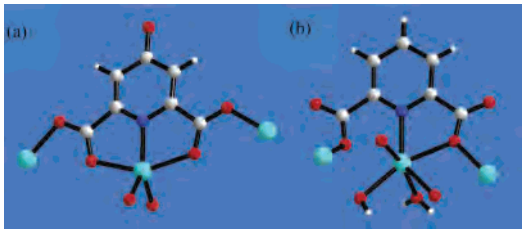

Figure 1. Coordination environment of **1** (a) and **1a** (b); red, O; white, H; gray, C; cyan, Zn; blue, N.

Results and Discussion

Structural Analysis of $\{[Zn(HCAM)]\cdot H_2O\}_n$ (1) and $\{[Zn(PDA)(H_2O)_{1.5}]\}_n$ (1a). The reaction of Zn(II) salts with H_3CAM and H_2PDA under hydrothermal conditions gave a 2D coordination polymer **1** and 1D coordination polymer **1a**, respectively. The Zn(II) ion is pentacoordinated with a distorted trigonal bipyramidal geometry in **1** (Figure 1a). The equatorial sites are occupied by an NO_2 donor from the carboxylate groups at the pyridine-2,6-position of HCAM. Two O atoms from two other neighboring HCAM ligands occupy the axial sites. The Zn−O distances range from 1.944 to 2.245 Å, which are within normal ranges found in other zinc complexes.[32] As shown in Figure 1b, three O atoms from different PDAs, one N atom, and two O atoms of terminal and bridged water molecules complete the six-coordinated environment of the metal center in **1a**. The Zn−O length of O from terminal water is smaller than that from bridged water and PDA molecules. The average Zn−O and Zn−N lengths are slightly larger than that in **1**, which may be due to the unusual coordination behavior of PDA. Each PDA can be described as asymmetric tetradentate buildings block (mode **H**) linking three Zn centers to form trinuclear units. The coordination mode **H** of PDA is first found.

As shown in Figure 2, each square grid with dimensions of 5.3 × 5.3 Å^2 is composed of four coplanar Zn(II) ions linked through four CAM molecules in **1**. The tetranuclear Zn_4 metallic rings are further connected by carboxylate O to form an infinite 2D grid with a (4,4) net. In **1a**, Zn(II) ions are linked via alternative single and double oxygen bridges to form a 1D zigzag chain, which give two kinds of Zn···Zn distances (3.699 and 3.346 Å).

The hydroxyl oxygen atoms in CAM do not coordinate to the metal centers, which direct the formation of hydrogen

(32) Ghosh, S. K.; Savitha, G.; Bharadwaj, P. K. *Inorg. Chem.* **2004**, *43*, 5495.

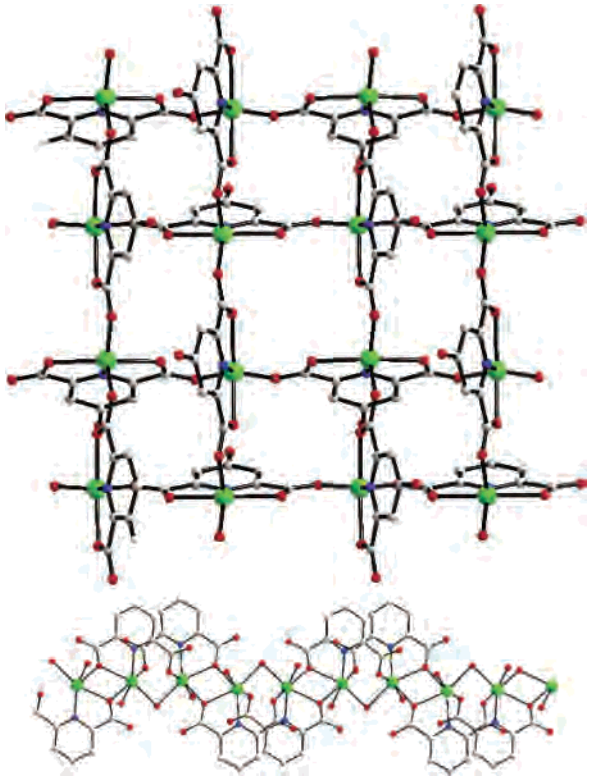

Figure 2. 2D (4,4) net linked via carboxylate groups of **1** along the *c* axis (top) and 1D chain of **1a** along the *a* axis (bottom). Green, Zn; red, O; gray, C; blue, N.

bonds with water molecules. The hydrogen bonds between carboxylate O atoms or OH groups and water molecules link the 2D coordination sheets to form a 3D supramolecular structure (Figure 3). The 2D coordination sheets pack in an ABAB sequence along the *c* direction with channels of the approximated dimensions 5×5 Å^2. For **1a**, each 1D chain links four other chains by hydrogen bonding between coordination water molecules and oxygen atoms of PDA, which results in a 3D supramolecular network. The pyridine rings of neighboring 1D chains are close. The packing motif in **1a** is unsuitable for the complex of H_3CAM because the stereochemical effect of the hydroxyl group prevents pyridine rings from packing closely.

Structural Analysis of $\{[Nd_2(HCAM)_3(H_2O)_4]\cdot 2H_2O\}_n$ (2) and $\{[Nd_2(PDA)_3(H_2O)_3]\cdot 0.5H_2O\}_n$ (2a). While we investigated the coordination chemistry of H_3CAM with Nd_2O_3, a 2D coordination polymer **2** was isolated. The single-crystal analysis of **2** reveals that Nd atoms have two types of coordination environments (Figure 4a). Nd1 is nine-coordinated with a tricapped trigonal prism geometry, whereas Nd2 is eight-coordinated. The Nd1 atom coordinates to three HCAM molecules by using six oxygen atoms and three nitrogen atoms to form a coordination sphere. The Nd2 atom coordinates to four HCAMs by using four oxygen atoms from carboxylate groups and four water molecules to complete the coordination geometry. The Ln(III)−O and Ln(III)−N distances are within normal ranges.[33] The distance between Nd1 and Nd2 atoms is 6.344(8) Å. Using H_2PDA instead of H_3CAM in the self-assembly system, we synthesized and analyzed the structure of **2a** independently in our lab, although Ghosh et al. reported the similar complex $[Nd_2(PDA)_3(H_2O)_3]_n$ with different lattice water molecules.[33] In this work, we introduced **2a** to compare study the coordination chemistry of H_3CAM and H_2PDA in the same M/ligand ratio and synthesized conditions. The asymmetric coordination unit of **2a** (Figure 4b) gives two independent lanthanum atoms Nd1 and Nd2. Nd1 is nine-coordinated, whereas Nd2 is eight-coordinated and resulting polyhedra are NdO_7N_2 and NdO_7N, respectively. There are three crystallographically independent PDA molecules in the structure with coordination motifs **C**, **E**, and **F**.

In **2**, the Nd1 and Nd2 atoms are alternately arrayed by carboxylate bridges and generate a tetranuclear homometallic Nd_4 square unit with 16-membered $Nd_4C_4O_8$ motifs. The Nd_4 square structure as a building block is further assembled into

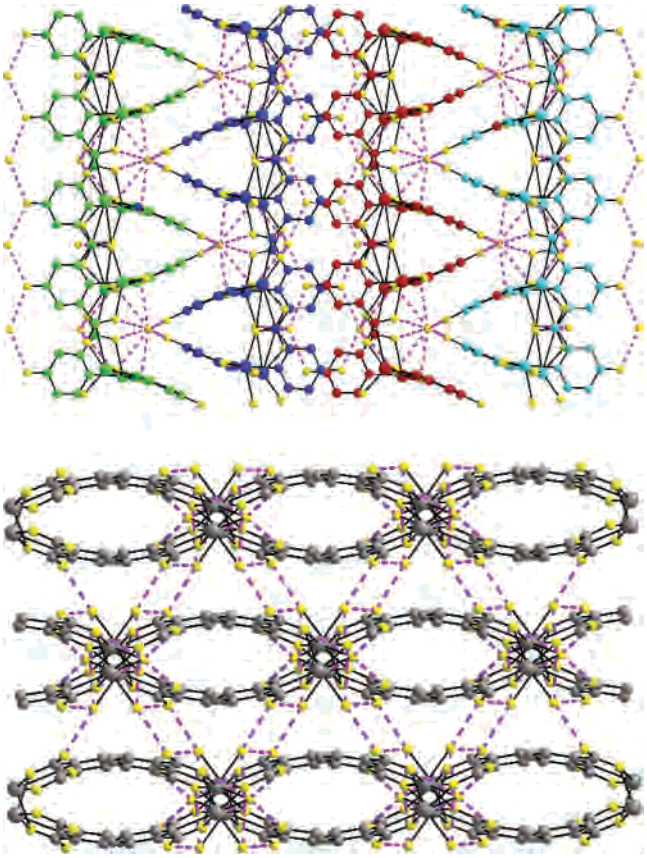

Figure 3. View of the ABAB packing structure along *b* of **1** along the *a* axis (top) and 3D supramolecular network of **1a** along the *c* axis (bottom). Yellow, O; other colors, different atoms with O in order to highlight the hydrogen bond; purple dot, O···O hydrogen bond; H atoms are omitted.

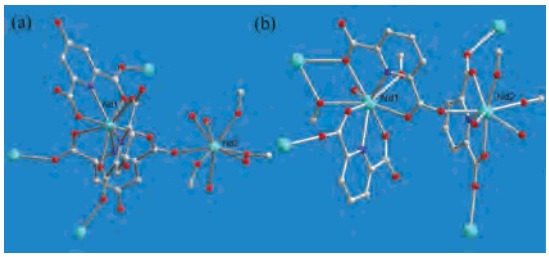

Figure 4. Coordination unit of **2** (a) and **2a** (b). Cyan, Nd; red, O; gray, C; blue, N.

(33) Ghosh, S. K.; Bharadwaj, P. K. *Inorg. Chem.* **2004**, *43*, 2293.

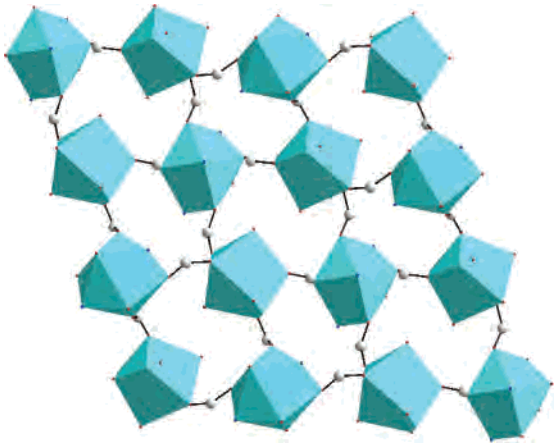

Figure 5. Diamond view of the 2D (4,4) grid motif in **2** along the *c* axis. Cyan, Nd; red, O; gray C; the H atoms and uncoordinated atoms of pyridine rings and hydroxyl groups are omitted.

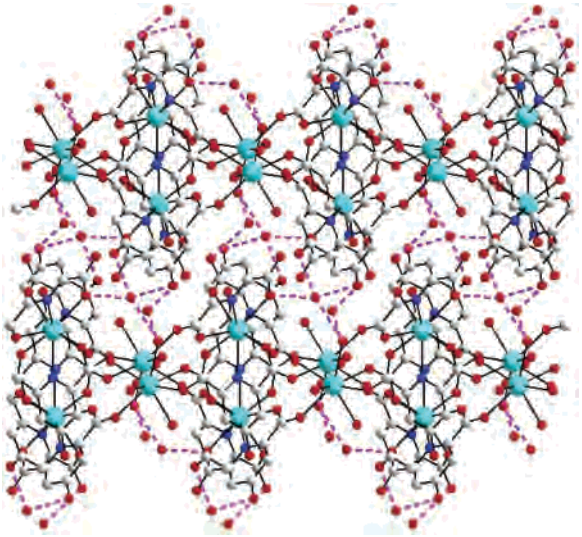

Figure 6. ABAB packing structure of **2** along the *b* axis. Cyan, Nd; red, O; blue, N; gray C; purple dot line, hydrogen bond; H atoms are omitted.

a highly ordered 2D grid (Figure 5). Various hydrogen bonds existed between water molecules and carboxylate O atoms or hydroxyl groups (Figure 6), as a result, the 2D grids are further assembled by hydrogen bonds to form a 3D supramolecular network. These hydrogen bonds help to stabilize the unusual topology of **2**. The 2D layers are packed in the ABAB sequence, and there are no open channels in **2**. In **2a**, the Nd1 and Nd2 atoms are alternately arrayed by carboxylate bridges to generate a 3D coordination polymer. The uncoordinated water molecules exist as guests in the micropores of the 3D network (Figure 7).

Structural Analysis of $\{[Gd(CAM)(H_2O)_3]\cdot H_2O\}_n$ (3). The self-assembly of H_3CAM with other Gd(III) salts gave a 2D coordination polymer **3**. The X-ray structural analysis reveals that **3** is monoclinic crystal system, space group $P2_1/n$. As shown in Figure 8, the center Gd(1) coordinates with one chelated tridentate CAM, two oxygen atoms from one carboxylate and one hydroxyl group, and three water molecules to form a $GdNO_7$ polyhedra. The Gd(III)−O distance (2.326 Å) between metal center and hydroxyl O atom are significantly shorter than these between Gd(1) and

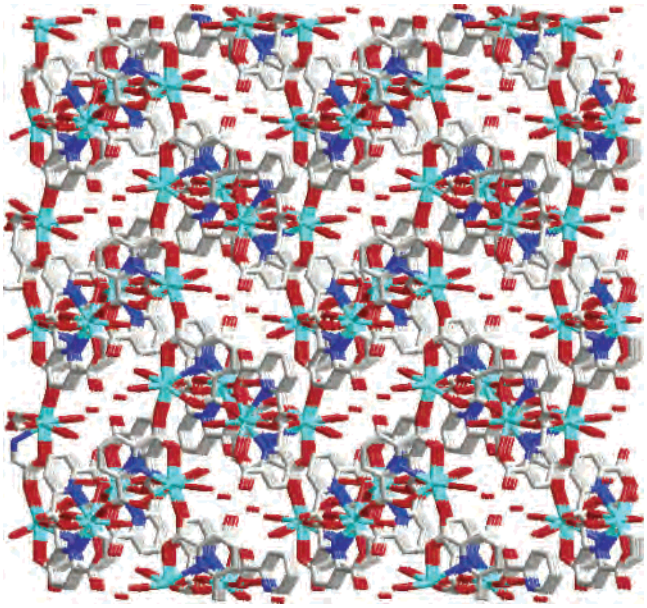

Figure 7. 3D open coordination network along the *a* axis in **2a**. Cyan, Nd; red, O; blue, N; gray C; red line, carboxylate group; H atoms are omitted.

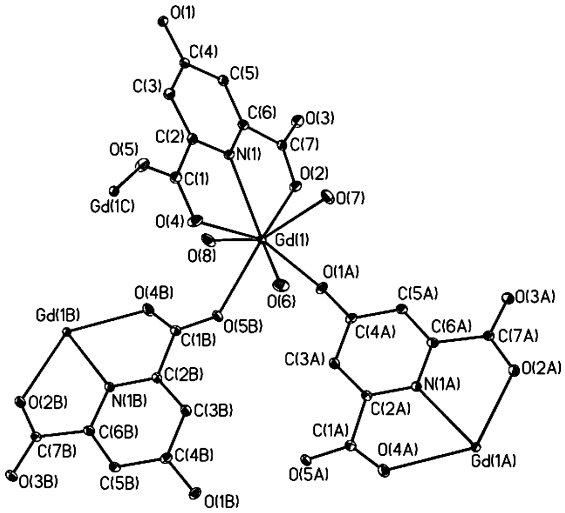

Figure 8. Coordination unit of **3**.

O atoms of carboxylate groups and water molecules. Each CAM acts as pentadentate ligand to link three different metal centers. As a result, two kinds of homometallic cycles $[Gd_4(CAM)_2]$ and $[Gd_4(CAM)_4]$ are constructed, resulting in different Gd···Gd distances (6.193 and 8.073 Å) in the cycles. The Gd_4 cycles as building blocks are further alternatively assembled into a highly ordered 2D grid (Figure 9). Each Gd(III) center can be considered as a five-connected node, and the topology of the 2D coordination sheet can be represented as a 3^34^2 uniform net. To our knowledge, **3** is the first example of the hydroxyl O coordinating with metal for the H_3CAM ligand.

Lanthanide Contraction. Compounds **3**−**5** are isomorphous. The various crystal lattice constants of these isomorphous complexes clearly exhibit the lanthanide contraction effect. The same effect is observed in **2** and **6** for the lattice constants. As shown in Table 3, the average Ln−O and Ln−N bond distances of **2**−**6** decrease with the series of

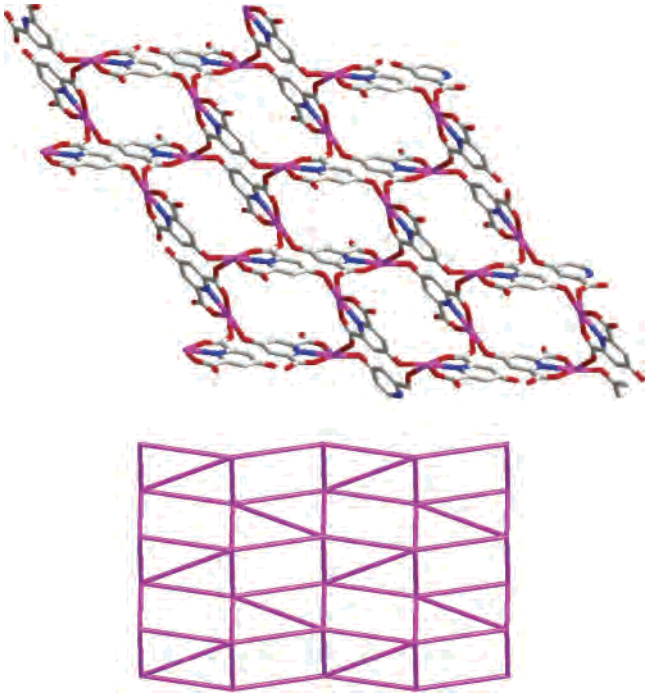

Figure 9. 2D coordination layer along the *a* axis (top) and 3^34^2 net (bottom) of **3**. Purple, Gd; gray, C; blue, N; red, O; H atoms are omitted; in the topology, Gd is shown as a node and the connectivity of the Gd centers by the organic ligand are shown as a line.

Table 3. Average Bond Lengths (Å) of Complexes **2**−**6** Based on H_3CAM[a]

	2 (Nd)	**3** (Gd)	**4** (Dy)	**5** (Er)	**6** (Er)
Ln−O_H		2.326	2.295	2.271	
Ln−O_W	2.491	2.406	2.370	2.348	2.358
Ln−O_C	2.473	2.430	2.404	2.385	2.392
Ln−N	2.566	2.493	2.460	2.441	2.452

[a] O_H, oxygen atom of the hydroxyl group; O_w, oxygen atom of the coordination water; O_C, oxygen atom of the carboxylate group.

Table 4. Reaction Conditions and Structures for **1**−**6**

	ligand	reactant	M/L ratio reactants	M/L ratio products	coordination modes of L	structure/ topology
1	H_3CAM	$ZnSO_4$	1:1	1:1	**E**−**1**	2D, (4,4) net
1a	H_2PDA	$ZnSO_4$	1:1	1:1	**H**	1D, zigzag
2	H_3CAM	Nd_2O_3	2:3	2:3	**C-1, E**−**1**	2D, (4,4) net
2a	H_2PDA	Nd_2O_3	2:3	2:3	**C, E, F**	3D open net
3	H_3CAM	$Gd(ClO_4)_3$	2:3	1:1	**J**	2D, 3^34^2 net
3a	H_2PDA	$Gd(ClO_4)_3$	2:3	2:3	**C, E, F**	3D open net
4	H_3CAM	$DyCl_3$	2:3	1:1	**J**	2D, 3^34^2 net
5	H_3CAM	$Er(ClO_4)_3$	2:3	1:1	**J**	2D, 3^34^2 net
6	H_3CAM	Er_2O_3	2:3	2:3	**C-1, E**−**1**	2D, (4,4) net

Nd to Er, where it was ascribed to crystal-field contractions of those rare earth ions lacking spherical symmetry.[34]

Investigation of the Reactions and Structures. The synthesized and structural details are summarized in Table 4. Using Nd_2O_3 and $Gd(ClO_4)_3$ in the similar synthesized system, we obtained **2** and **3** with different coordination networks and M/L ratio in the products. However, the reactions of H_2PDA and Ln(III) salts or Ln_2O_3 produced the similar MOFs. The results reply that oxides and salts give different self-assemble processes for H_3CAM. The hydroxyl groups in H_3CAM have relatively less acidity than carboxylate groups, which react with Ln(III) ions but cannot react with Ln_2O_3. As a result, the Er(III) complexes **5** and **6** exhibit different coordination networks. In H_2PDA, the carboxylate groups can react with both Ln(III) salts or Ln_2O_3, which gave the similar coordination products for **2a** and **3a**. Though different anions were employed in the self-assembly of H_3CAM and Ln(III), the similar 2D MOF was obtained for **3** and **4**.

Compared with H_2PDA, the introduction of a hydroxyl group in H_3CAM resulted in three effects: (i) a supramolecular effect, namely, providing hydrogen-bonding donor or acceptor sites in the construction of supramolecular packing; (ii) a coordinated effect, namely, adding a coordination sites to link more metal centers, and (iii) a stereochemical effect. Though **1** and **1a** were synthesized under similar conditions, the dramatic change of the structures from 1D (**1a**) to 2D (**1**) and different coordination motifs for multicarboxylic ligands are due to (i) and (iii). The stereochemical effect of the hydroxyl group is the main reason in the self-assembly of Nd_2O_3 and H_3CAM in the M/L ratio of 2:3 to result in 2D rather than 3D MOFs for **2**.

IR Spectra. The IR spectra of **1**−**3** show broad peaks in the range of 3600−3200 cm^{-1} due to the existence of hydrogen bonding between water molecules. In the middle of the stretching vibrations, the IR results are employed to distinguish the coordination modes of carboxylate groups. A correlation of the carboxylate coordination mode to metal ions was made by examining the difference $\Delta\nu$ ($\nu_{as} - \nu_s$) of the complexes.[35] The vibrations of $\nu_{as}(CO_2^-)$ and $\nu_s(CO_2^-)$ are at 1638.3, 1622.1, and 1469.7 cm^{-1} for **1**. Compared with **1**, $\nu_{as}(CO_2^-)$ is at 1614.7 cm^{-1} and $\nu_s(CO_2^-)$ is at 1462.9 and 1396.7 cm^{-1} for **1a**, which indicate that CAM functions in a bidentate motif and PDA functions in both monodentate and bidentate motifs. The $\Delta\nu$ values for **2**, **2a**, and **3** show the presence of monodentate and bidentate motifs. The absence of the characteristic bands at around 1700 cm^{-1} in **1**−**3** indicates the complete deprotonation of carboxylate groups in H_3CAM and H_2PDA upon reaction with the metal ions.

TGA. TGA was carried out for polycrystalline samples of compounds **1**−**3** in the temperature range 25−550 °C (Figure 10). For **1**, the first weight loss of 7.1% in the range of 50−208 °C corresponds to the loss of one uncoordinated water molecule (calcd 6.8%). The second weight loss above 408 °C corresponds to the decomposition of the coordination network. The weight loss of water molecules is in the temperature range 100−220 and 80−180 °C for **2** and **3**, respectively, and then the compounds continued to decompose above this temperature and complete decomposition is not achieved above 550 °C. For **1a**, the first weight loss 11.1% is between 100 and 147 °C, which is attributed to the loss of water molecules (calcd 10.5%). The second weight loss, 35.5% occurred from 222 to 267 °C, and the product began to lose both carboxylate groups of the ligand (calcd

(34) Yao, J.; Deng, B.; Sherry, L. J.; McFarland, A. D.; Ellis, D. E.; Duyne, R. P. V.; Ibers, J. A. *Inorg. Chem.* **2004**, *43*, 7735.

(35) Nakamoto, K. *Infrared and Raman Spectra of Inorganic and Coordination Compounds*; John Wiley and Sons: New York, 1997.

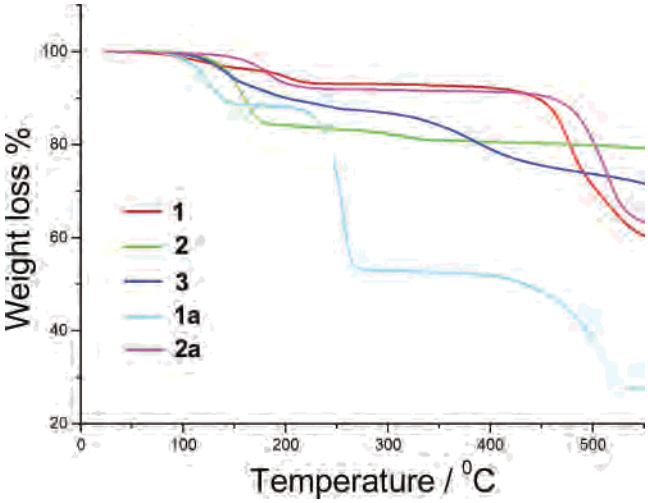

Figure 10. TGA curves.

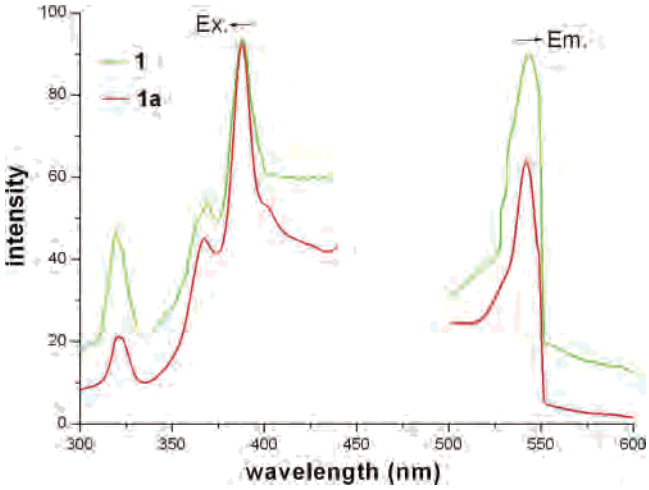

Figure 11. Exication and emission spectra in the solid state of **1** and **1a**.

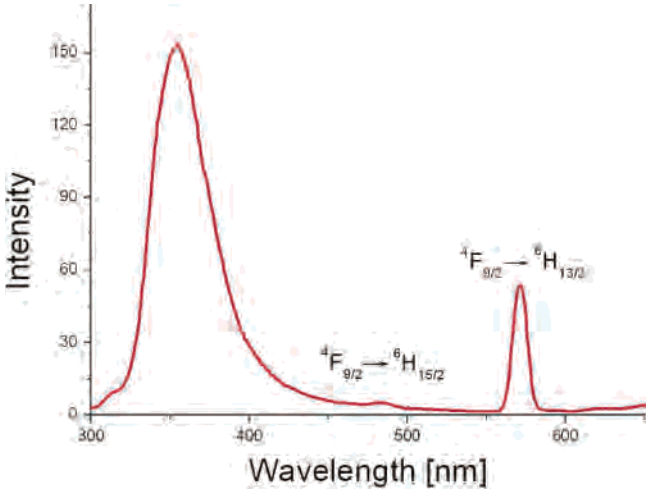

Figure 12. Emission spectra of **4** in DMF solution (10^{-3} mol L^{-1}) excited at 282 nm.

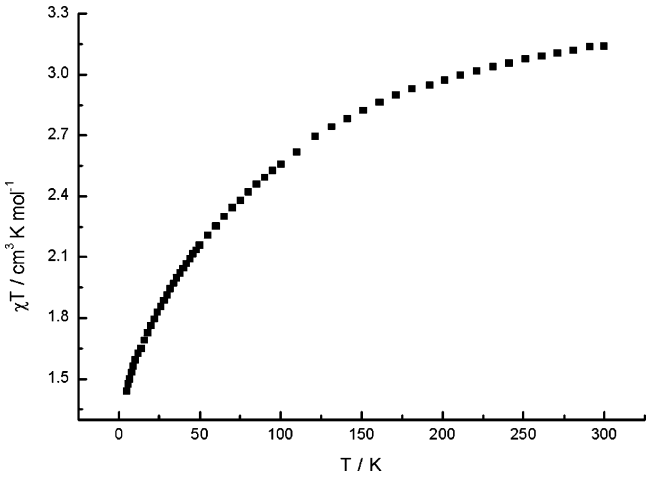

Figure 13. Plot of $\chi_M T$ vs T for **2**.

34.9%). Above this temperature, the compound continues to decompose. TGA of **2a** shows that the onset of weight loss occurs above 150 °C, which shows that H_2O molecules are tightly held in the 3D MOF. The decomposition for the MOF begins above 450 °C. The TGA results show that the 1D complex **1a** is more unstable than 2D and 3D complexes, and the 3D MOF (**2a**) normally show**s** high robustness for the coordination networks.

Luminescent Properties. The excitation and emission spectra of **1** and **1a** in the solid state at room temperature are depicted in Figure 11. Both **1** and **1a** exhibit strong green emission with $\lambda_{max} = 543$ nm while excitation at 388 nm. The strongest emission peaks for H_2PDA and H_3CAM are both at about 319 nm, which is due to the $\pi-\pi^*$ and/or $\pi^* \rightarrow n$ transition.[30] Compared with the ligands, the large red-shift of intraligand fluorescence in **1** and **1a** is probably due to the ligand-to-metal charge transfer (LMCT). The fluorescence efficiency for **1** is higher than that for **1a**, which may be due to different coordination environments around the metal centers.

The emission spectra of **4** at room temperature in DMF solution excited at 282 nm are shown in Figure 12. The board and strong emission bands in 320−380 nm are due to the $\pi^* \rightarrow \pi$ or $\pi^* \rightarrow n$ transition of organic ligands. The emissions at 483 and 571 nm are due to $^4F_{9/2} \rightarrow {}^6H_{15/2}$ and $^4F_{9/2} \rightarrow {}^6H_{13/2}$ of the Dy^{3+} ion.[36] The relatively low emission intensity for Dy(III) ions imply that the efficiency of energy-transfer from ligands to metals is low.

Magnetic Properties. The $\chi_M T$ vs T curve of **2** is shown in Figure 13. The effective magnetic moment of the Nd^{3+} ion at room temperature is 3.15 cm^3 K mol^{-1}, which is close to the theoretical value of 3.28 cm^3 K mol^{-1} for the free Nd^{3+} ion. The $\chi_M T$ value decreases continuously to a value of 1.45 cm^3 K mol^{-1} at 4 K. It is noted that the $4f^n$ configuration of a Ln(III) ion is split into $^{2S1+}L_J$ states by the interelectronic repulsion and the spin−orbit coupling. Further splitting into Stark components is caused by the crystal-field perturbation, which depends on the symmetry site of the ion.[37] At room temperature, all the Stark levels arising from the 10-fold degenerate $^4I_{9/2}$ ($S = 3/2$, $J = 9/2$) ground states of Nd^{III} ion are populated, but as the temperature decreases, a progressive depopulation of these levels

(36) Tedeschi, C.; Azema, J.; Gornitzka, H.; Tisnes, P.; Picard, C. *Dalton Trans.* **2003**, 1738.
(37) Bunzli, J.-C. G.; Chopin, G. R. *Lanthanide probes in Life, Chemical and Earth Sciences*; Elsevier: Amsterdam, 1989.

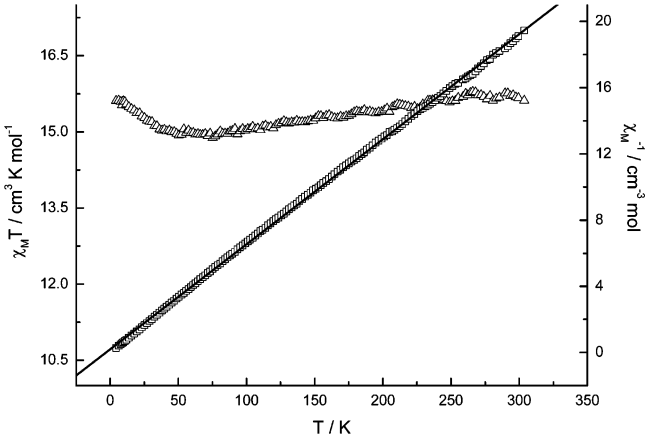

Figure 14. Plots of $\chi_M T$ and χ_M^{-1} vs T for **3a**.

occurs. As a result, the nature of the interactions between the two Nd(III) ions with an orbital momentum cannot be unambiguously deduced only from the shape of the $\chi_M T$ vs T curve.

The variations of the inverse of the magnetic susceptibility, χ_M^{-1}, and $\chi_M T$ of **3a** are shown in Figure 14. The thermal evolution of χ_M^{-1} obeys the Curie−Weiss law, $\chi_M = C/(T - \theta)$, over the whole temperature range with a Weiss constant, θ, of −3.07 K. The Curie constant, C, of 15.755 cm^3 K mol^{-1} is consistent with the expected value for two isolated Gd.[38] The $\chi_M T$ at 300 K is 15.67 cm^3 K mol^{-1}, which is close to the value for two isolated Gd^{3+} ions ($^8S_{7/2}$). When the temperature is lowered, $\chi_M T$ decreases slightly to 14.9 cm^3 K mol^{-1} at 65 K and then increases below 65 K to 15.7 cm^3 K mol^{-1} at 5 K. Because the factors governing the nature and magnitude of the Gd···Gd interactions are complicated in the 3D MOF of **3a**, the quantitative analysis of the magnetic susceptibility is difficult.

(38) Lai, W. P. W.; Wong, W. T.; Li, B. K. F.; Cheah, K. W. *New J. Chem.* **2002**, *26*, 576.

Conclusion

In summary, the first contrastive study for the coordination chemistry of H_3CAM and H_2PDA based on a series of MOFs was reported. **1** is a 2D (4,4) net, and **1a** is a 1D zigzag chain connected via alternatively single and double O bridges. **2** and **6** contain a highly ordered 2D (4,4) grid, while **2a** and **3a** are 3D open networks. **3**−**5** are 2D polymers with a 3^34^2 uniform net, where hydroxyl groups of H_3CAM coordinate with metal ions. The coordination modes of PDA and CAM are summarized, and modes **H** and **J** are first found in this contribution. The stereochemical and supramolecular effects of the hydroxyl group result in the dramatic structural change from 1D (**1a**) to 2D (**1**) and from 2D (**2**) to 3D (**2a**). The hydroxyl groups in H_3CAM can only react with Ln(III) salts, which result in two kinds of isomorphous compounds (**3**−**5**) and (**2**, **6**). Complexes **1** and **1a** exhibit strong green fluorescent emission bands, and **4** exhibits emissions for ligands and Dy(III) centers, which renders them potential use as fluorescent materials.

Acknowledgment. This work was supported by the National Natural Science Foundation of China (Grants No. 90501002, 20501012, and 20425103) and the National Key Project for Fundamental Research (2005CCA01200).

Supporting Information Available: Crystallographic data of **1**−**6** in CIF files. This material is available free of charge via the Internet at http://pubs.acs.org.

IC060550J